Journal of Molecular Histology (2018) 49:99–110
https://doi.org/10.1007/s10735-017-9750-3

ORIGINAL PAPER

Ca^{2+}-CaMKKβ pathway is required for adiponectin-induced secretion in rat submandibular gland

Chong Ding[1] · Zhi-Hao Du[2] · Sheng-Lin Li[1] · Li-Ling Wu[3] · Guang-Yan Yu[2]

Received: 13 November 2017 / Accepted: 5 December 2017 / Published online: 14 December 2017

Abstract

Adiponectin functions as a promoter of saliva secretion in rat submandibular gland via activation of adenosine monophosphate-activated protein kinase (AMPK) and increased paracellular permeability. Ca^{2+} mobilization is the primary signal for fluid secretion in salivary acinar cells. However, whether intracellular Ca^{2+} mobilization is involved in adiponectin-induced salivary secretion is unknown. Here, we found that full-length adiponectin (fAd) increased intracellular Ca^{2+} and saliva secretion in submandibular glands. Pre-perfusion with ethylene glycol-bis (2-aminoethylether)-*N,N,N′,N′*-tetraacetic acid (EGTA) combined with thapsigargin (TG), an endoplasmic reticulum Ca^{2+}-ATPase inhibitor, abolished fAd-induced salivary secretion, AMPK phosphorylation, and enlarged tight junction (TJ) width. Furthermore, in cultured SMG-C6 cells, co-pretreatment with EGTA and TG suppressed fAd-decreased transepithelial electrical resistance and increased 4-kDa FITC-dextran flux responses. Moreover, fAd increased phosphorylation of calcium/calmodulin-dependent protein kinase (CaMKKβ), a major kinase that is activated by elevated levels of intracellular Ca^{2+}, but not liver kinase B1 phosphorylation. Pre-perfusion of the isolated gland with STO-609, an inhibitor of CaMKKβ, abolished fAd-induced salivary secretion, AMPK activation, and enlarged TJ width. CaMKKβ shRNA suppressed, whereas CaMKKβ re-expression rescued fAd-increased paracellular permeability. Taken together, these results indicate that adiponectin induced Ca^{2+} modulation in rat submandibular gland acinar cells. Ca^{2+}-CaMKKβ pathway is required for adiponectin-induced secretion through mediating AMPK activation and increase in paracellular permeability in rat submandibular glands.

Keywords Adiponectin · Calcium · Calcium/calmodulin-dependent protein kinase · Adenosine monophosphate-activated protein kinase · Submandibular gland · Secretion

Introduction

Saliva is important for the initiation of digestion and the maintenance of oral health. Severe hyposalivation leads to dental caries, oral pain and mucosal infections (Kaplan and Baum 1993). Saliva secretion is accomplished through the interaction of autonomic neurotransmitters with their respective receptors (i.e., muscarinic acetylcholine cholinergic, α-adrenergic, and β-adrenergic receptors) on gland acinar cells (Baum 1993). Besides, there is increasing evidence that salivary secretion is also evoked by non-cholinergic or non-adrenergic pathways that utilize neuropeptides, such as substance P and neuropeptide Y, as well as other molecules released by nerve terminals (Garrett et al. 1999). In the previous study, we reported that adiponectin, an adipokine, promotes salivary secretion in rat submandibular glands via activation of adenosine monophosphate activated protein

✉ Li-Ling Wu
pathophy@bjmu.edu.cn

✉ Guang-Yan Yu
gyyu@263.net

[1] Center Laboratory, Peking University School and Hospital of Stomatology, Beijing 100081, People's Republic of China

[2] Department of Oral and Maxillofacial Surgery, Peking University School and Hospital of Stomatology, 22 Zhongguancun South Street, Haidian District, Beijing 100081, People's Republic of China

[3] Department of Physiology and Pathophysiology, Peking University School of Basic Medical Sciences, Key Laboratory of Molecular Cardiovascular Sciences, Ministry of Education, and Beijing Key Laboratory of Cardiovascular Receptors Research, 38 Xueyuan Road, Haidian District, Beijing 100191, People's Republic of China

kinase (AMPK) and increased paracellular permeability (Ding et al. 2013).

Ca^{2+} mobilization plays a crucial role in saliva secretion. For example, activation of muscarinic cholinergic receptors (mAChRs) rapidly triggers the release of intracellular Ca^{2+} ($[Ca^{2+}]_i$) from endoplasmic reticulum (Coronado et al. 1994; Joseph 1996), which subsequently evokes influx of Ca^{2+} from the extracellular medium, resulting in a sustained increase in $[Ca^{2+}]_i$ (Liu et al. 1998). The increase in $[Ca^{2+}]_i$ in turn causes the opening of Ca^{2+}-gated K^+ and Cl^- channels (Giovannucci et al. 2002; Nauntofte and Poulsen 1986; Nehrke et al. 2003), and up-regulates $Na^+/K^+/2Cl^-$ cotransporter (Evans and Turner 1997), Na^+/H^+, and Cl^-/HCO_3^- exchangers (Manganel and Turner 1990; Nguyen et al. 2004). Furthermore, increased $[Ca^{2+}]_i$ induces aquaporin 5 trafficking, resulting in the forming of water pores that facilitates the rapid increase in transcellular water permeability (Ishikawa et al. 1998). However, adiponectin-promoted saliva secretion in rat submandibular glands is independent of mAchRs (Ding et al. 2013). Whether Ca^{2+} mobilization is involved in adiponectin-induced salivary secretion is unknown.

AMPK plays a key role in adiponectin-mediated metabolic modulation and cardiovascular protection (Shibata et al. 2005; Yamauchi et al. 2002). Activation of AMPK is controlled by two upstream kinases, liver kinase B1 (LKB1) and calcium/calmodulin-dependent protein kinase (CaMKKβ) (Hawley et al. 2005; Woods et al. 2003). LKB1 has been considered as a constitutively serine/threonine protein kinase that is ubiquitously expressed in mammalian cells, and phosphorylates the catalytic subunit of AMPK by increasing cellular AMP:ATP ratio (Hawley et al. 2003). In contrast, the activation of AMPK by CaMKKβ is initiated by an increase in $[Ca^{2+}]_i$, but not affected by changes in the ATP:AMP ratio (Woods et al. 2005). To date, whether LKB1 and/or CaMKKβ are involved in the adiponectin-mediated AMPK activation and saliva secretion in submandibular gland is not clarified.

Thus, the present study was designed to explore the role of adiponectin-induced intracellular Ca^{2+} mobilization in salivary secretion and its underlying mechanism. These findings will improve our understanding of the biological roles of adiponectin and Ca^{2+} in saliva secretion, and provide a potential therapeutic strategy for the treatment of submandibular gland dysfunction.

Materials and methods

Animal ethics

Healthy male Sprague Dawley (SD) rats weighing 250–270 g each were obtained from the Peking University Health Science Center. All experimental procedures and procedures for the care and use of the animals were approved by the Peking University Institutional Review Board. All surgical procedures were performed under chloral hydrate anesthesia (400 mg/kg body weight), and all efforts were made to minimize the animals' suffering.

Reagents and antibodies

Rat recombinant full length adiponectin (fAd), ethylene glycol-bis (2-aminoethylether)-*N,N,N′,N′*-tetraacetic acid (EGTA), thapsigargin (TG), and STO-609 were purchased from Sigma-Aldrich (St. Louis, MO, USA). Antibodies against CaMKKβ, p-LKB1, and LKB1 (Cat. Nos. sc-271924, sc-32245, and sc-50341, respectively) were from Santa Cruz Biotechnology (Carlsbad, CA, USA). Antibodies against p-CaMKKβ, p-AMPK, and AMPK (Cat. #12818, #2531, and #2532, respectively) were from Cell Signaling Technology (Danvers, MA, USA). Antibody against glyceraldehyde-3-phosphate dehydrogenase (GAPDH) (Cat. No. M2006) was from Abmart (Shanghai, China). Other chemicals and reagents were of analytical grade.

Rat submandibular gland acinar cell preparation

Primary isolated rat submandibular gland acinar cells were prepared by enzymatic digestion according to the method (Zhang et al. 1996, 2006) with minor modifications. Briefly, rat submandibular gland tissues were excised and dissected free of connective tissue, rinsed twice with ice-cold phosphate-buffered saline (PBS), cut into small pieces, and digested in medium containing 100 units/ml of collagenase (Worthington, Lakewood, UK) and 1% BSA for 60 min. The digestion was terminated and washed twice with Dulbecco's modified Eagle's media (DMEM) containing 5% fetal bovine serum (FBS) and centrifuged at 1000*g* for 5 min. The cells were then resuspended in DMEM containing 15% FBS and filtered through a single layer of nylon bolting cloth (150 mesh).

Measurement of $[Ca^{2+}]_i$

Primary isolated acinar cells were loaded with Ca^{2+}-sensitive fluorescent probe fluo-2/AM (Thermo Fisher Scientific, MA, USA) for 30 min at 37 °C. Excitation was performed at 488 nm and the emission signals were collected through a 515 nm barrier filter. Images were taken every 10 s, and quantitated by average fluorescence intensities in randomly selected three to five cells in each time point from five submandibular gland cells (Carl Zeiss LSM710, Gottingen, Germany).

Perfusion of isolated rat submandibular glands

The effect of adiponectin on the secretory function of submandibular glands was measured according to the methods described previously (Ding et al. 2013). Briefly, after anesthesia, the submandibular glands were isolated and perfused through a polyethylene cannula placed in the external carotid artery. The main excretory duct was cannulated for saliva collection. Krebs-Ringer-HEPES (KRH, 116 mM NaCl, 5.4 mM KCl, 1.25 mM $CaCl_2$, 0.4 mM $MgSO_4$, 20 mM HEPES, 0.9 mM Na_2HPO_4, and 5.6 mM glucose, pH 7.4) buffer was warmed to 37 °C, bubbled with 95% O_2 and 5% CO_2, and perfused through the glands at a rate of 1.8 ml/min using a Gilson Minipuls rotary pump. After equilibration for at least 30 min, the glands were perfused with various stimulators or inhibitors (n = 8 for each group) for 10 min. Secretion by the glands was measured as the length of a column of moisture on a piece of filter paper (35 mm × 5 mm). In each group, salivary flow rates of perfused glands were measured. Then gland tissues were collected and analyzed by Western blot and transmission electron microscopy.

Cell culture

The rat submandibular gland cell line SMG-C6 (a generous gift from Dr. David O. Quissell without commercial purpose) was routinely grown at 37 °C in a humidified 5% CO_2 atmosphere in DMEM/F12 (1:1 mixture) medium containing 2.5% FBS, 5 mg/ml transferrin, 1.1 mM hydrocortisone, 0.1 mM retinoic acid, 2 nM thyronine T3, 5 mg/ml insulin, 80 ng/ml epidermal growth factor, 50 mg/ml gentamicin sulfate, 5 mM glutamine, 100 U/ml penicillin, and 100 mg/ml streptomycin (Quissell et al. 1997). All constituents used in culturing SMG-C6 cells were purchased from Sigma-Aldrich Co.

Western blot analysis

The cultured cells were homogenized in lysis buffer (50 mM Tris–HCl, 150 mM NaCl, 1 mM EDTA, 1 mM phenylmethylsulfonyl fluoride, 1% Triton X-100, 0.1% SDS, and 0.1% sodium deoxycholate, pH 7.2) using a polytron homogenizer as previously described (Ding et al. 2013). The homogenates were centrifuged at 12,000*g* for 10 min at 4 °C. The protein concentration of the supernatant was measured by the Bradford method. Equal amounts of proteins (20 μg) from each sample were separated on 12% SDS-PAGE and electroblotted on polyvinylidene fluoride membranes. The blocked membranes were incubated with antibodies against p-CaMKKβ (1:1000), CaMKKβ (1:400), p-LKB1 (1:600), LKB1 (1:600), p-MAPK (1:1000), AMPK (1:1000), or GAPDH (1:4000), respectively. The blots were then probed with horseradish peroxidase-conjugated secondary antibodies (ZSGBBIO, Beijing, China), and the target proteins were detected using enhanced chemiluminescence reagent (Pierce Biotechnology, Rockford, IL, USA). GAPDH was used as a loading control.

Transmission electron microscopy

The gland specimens were fixed in 2% paraformaldehyde-1.25% glutaraldehyde. Ultrathin sections were stained with uranyl acetate and lead citrate and examined with a transmission electron microscope (H-7000, HITACHI, Tokyo, Japan). Each image was obtained under the same conditions of brightness and contrast to permit comparison of tight junction (TJ) density among the different groups. For morphometric analysis, the distances between neighboring TJs (shown as the width of the apical TJs) were measured and averaged in ten randomly selected fields in each of four sections by two blinded examiners using ImageJ software (NIH, MD, USA) as previously described (Ding et al. 2013).

Knockdown and re-expression of CaMKKβ

SMG-C6 cells were cultured to 80% confluence and transfected with shRNA of interest using MegeTran 1.0 (Origene, MD, USA) according to the manufacturer's instructions. For knockdown of CaMKKβ, CaMKKβ shRNA (CAGCGACGC CTTGCTGTCTAACACCGTGG) and a scrambled control were constructed in pGFP-V-RS vectors and synthesized by Origene Technologies.

CaMKKβ re-expression ('rescue') was conducted by generating a Myc-tagged cDNA clone of CaMKKβ in a pCMV6 vector (Origene). Plasmid transfection was performed using MegeTran 1.0 at a transfection reagent: DNA ratio which was 3:1 as described in the manufacturer's instructions. The cells were collected 24 h post-transfection.

Transepithelial electrical resistance measurement and paracellular tracer flux assay

Confluent monolayers of SMG-C6 cells were grown in 24-well Corning Transwell™ chambers (polycarbonate membrane, filter pore size 0.4 μm, area 0.33 cm^2; Costar) for 7 days, transepithelial electrical resistance (TER) was then measured at 37 °C using an epithelial volt ohm meter (EVOM; WPI, FL, USA). TER values were calculated by subtracting the blank filter (90 Ω) and by multiplying by the surface area of the filter. All measurements were performed on a minimum of three wells.

For paracellular tracer flux assay, 1 mg/ml 4-kDa FITC-dextran was added to the medium at the apical sides of the chambers, and the samples were collected from the basal sides of the chambers after incubation for 3 h. The apparent permeability coefficient (*P*app) was determined as the

increase in the amount of tracer per time per filter area by using a fluorometer (BioTek, VT).

Statistical analysis

Data are presented as the mean ± SD. Statistical analysis among multiple groups was performed by one-way ANOVA followed by Bonferroni's test using GraphPad software (GraphPad Prism, CA, USA). $P < 0.05$ was considered statistically significant.

Results

Effect of adiponectin on Ca^{2+} mobilization in isolated submandibular gland cells

Ca^{2+} was an important molecule in gland secretion. To reveal whether adiponectin could modulate Ca^{2+} in rat submandibular gland, we isolated rat submandibular glands acinar cells. As shown in Fig. 1a, b μg/ml fAd caused an increase in $[Ca^{2+}]_i$ of isolated submandibular gland acinar cells, and the increased $[Ca^{2+}]_i$ could last for more than 5 min.

Ca^{2+} is required for adiponectin-induced secretion in submandibular glands

To identify the role of Ca^{2+} in the secretion induced by adiponectin, we performed ex vivo perfusion of isolated rat submandibular glands. The basal saliva flow during KRH perfusion was 3.41 ± 1.29 mm/5 min, which was consistent with previous study (Ding et al. 2013). 1 μg/ml fAd significantly increased salivary flow rate by 289.62%. Pre-perfusion with EGTA (1 mM), a Ca^{2+} chelator, or TG (1 μM), an endoplasmic reticulum Ca^{2+}-ATPase inhibitor, alone did not reduce fAd-induced increase in salivary secretion. However, pre-perfusion with EGTA combined with TG abolished fAd-induced secretion. EGTA and/or TG alone had no effect on the basal saliva flow (Fig. 1c).

Next, we measured CaMKKβ and AMPK phosphorylation in these perfused glands (Fig. 1d). Compared with the KRH perfused glands, the levels of p-CaMKKβ in fAd-perfused glands with or without EGTA or TG were increased by 162.83, 143.61, and 173.46%, respectively. However, pre-perfusion with EGTA combined with TG abolished fAd-induced increased CaMKKβ phosphorylation. Perfusion with EGTA and/or TG alone did not affect the basal level of p-CaMKKβ (Fig. 1e). With the same tissues, the levels of p-AMPK in fAd-perfused glands with or without EGTA or TG were increased by 230.41, 214.73, and 208.39%, respectively, as compared with the KRH perfused gland. Pre-perfusion with EGTA combined with TG abolished fAd-induced increase in AMPK phosphorylation, whereas perfusion with EGTA and/or TG alone did not affect the basal level of p-AMPK (Fig. 1f). These results suggest that Ca^{2+} mobilization is required for adiponectin-induced salivary secretion, CaMKKβ and AMPK activation in rat submandibular glands. Both influx of extracellular Ca^{2+} and release of Ca^{2+} from endoplasmic reticulum might involve in these processes.

Ca^{2+} is involved in adiponectin-modulated tight junction ultrastructure

TJs are specialized structures located in the apical regions of lateral membranes between neighboring cells, establishing a barrier to the diffusion of solutes through paracellular pathway (Tsukita et al. 2001). To explore the possible role of Ca^{2+} in the paracellular pathway regulated by adiponectin, we examined the morphology of TJs in perfused glands under transmitted electron microscope. TJs were located in the apical portions of lateral membranes in acini, forming a slightly opened paracellular channel in unperfused submandibular glands (Fig. 2a) and were not affected by KRH perfusion (Fig. 2b). Perfusion with fAd increased TJ distance between neighboring epithelial cells (Fig. 2c), consistent with our previous findings (Ding et al. 2013). Pre-treatment with EGTA or TG did not affect the increase in TJ width induced by fAd (Fig. 2d, e). However, pre-treatment with EGTA combined with TG suppressed fAd-induced increase in TJ width (Fig. 2f). EGTA and/or TG alone had no influence on TJ ultrastructure (Fig. 2g–i).

Quantitative analysis showed that the average width of apical TJs was 11.34 ± 0.04 nm in KRH-perfused glands, similar with that in unperfused glands. The width of apical TJs was increased by 105.35% in fAd-perfused glands, by 113.64% in glands pre-prefused with EGTA, and by 102.48% in glands pre-treated with TG, compared with the KRH perfused glands. Pre-prefusion with EGTA combined with TG suppressed the increase in TJ width induced by fAd, whereas EGTA and/or TG alone had no effect on the basal TJ width (Fig. 2j). These results suggest that Ca^{2+}, including both extracellular Ca^{2+} influx and Ca^{2+} released from endoplasmic reticulum, are involved in the "opening" of TJs regulated by adiponectin in submandibular glands.

Ca^{2+} contributes to the adiponectin-modulated paracellular permeability

We previously found that the adiponectin-induced saliva secretion in rat submandibular glands was accomplished by an increase in epithelial paracellular permeability (Ding et al. 2013). To determine whether Ca^{2+} is involved in the regulation of paracellular permeability by adiponectin, we performed TER measurement on monolayers of polarized

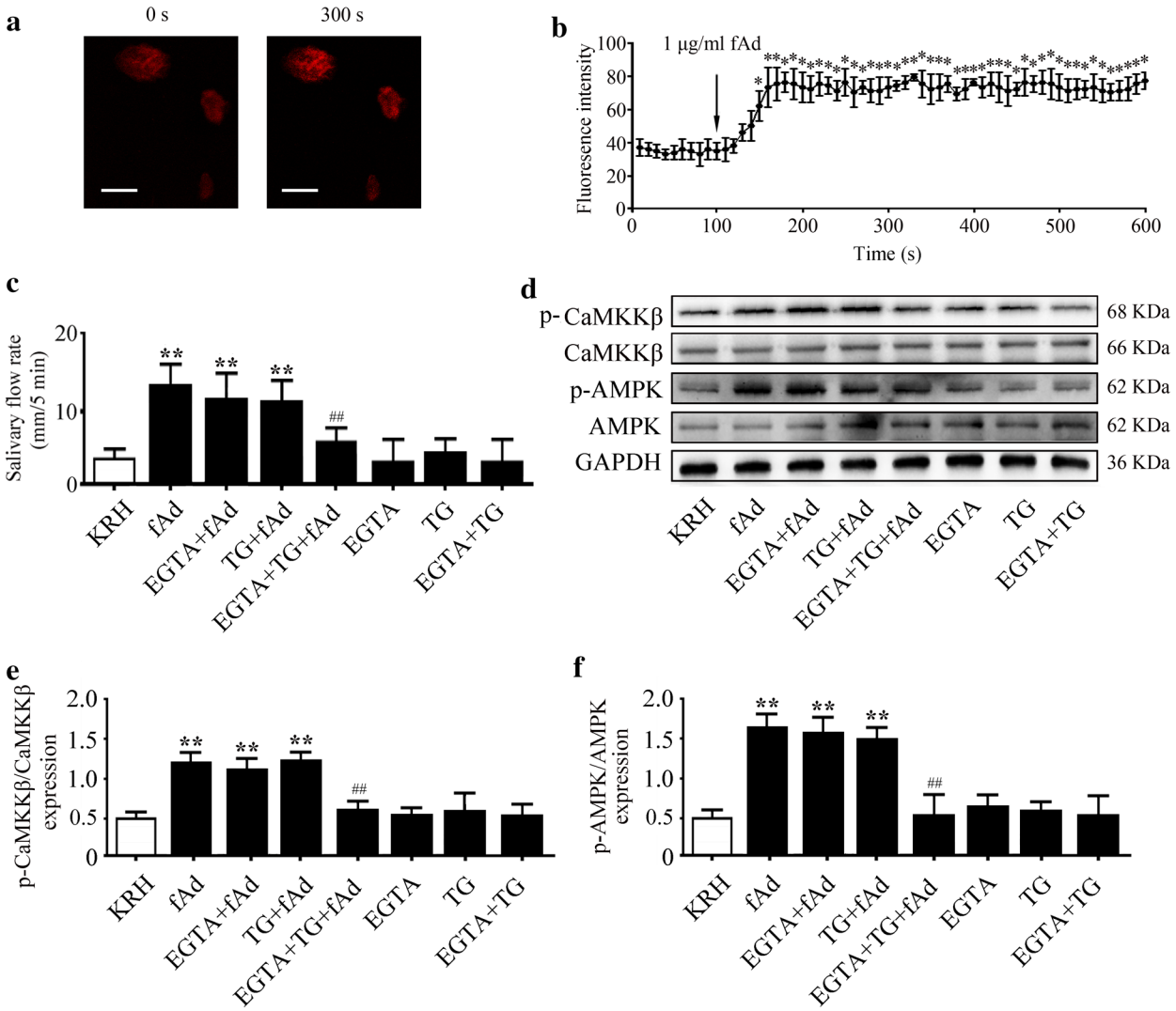

Fig. 1 Ca^{2+} mobilization is required for adiponectin-induced secretion in submandibular glands. **a** Representative fluorescence image of furo-2/AM-loaded cells before (left) and after (right) stimulation with 1 μg/ml fAd. Bar: 20 μm. **b** Quantitative analysis fluorescence intensities of submandibular cells stimulated by 1 μg/ml fAd and the time-course. Arrows denote the time of fAd application. The values shown are means ± SD from five independent experiments. $^{*}P < 0.05$ compared with the average intensities of untreated cells. Isolated rat submandibular glands were perfused with Krebs–Ringer–HEPES (KRH), and salivary flow rates were measured after equilibration for 30 min, perfusion with stimulators or inhibitors for 10 min. **c** The salivary flow rate in glands perfused with KRH for 10 min, perfused with 1 μg/ml fAd for 10 min, pre-perfused with 1 μM EGTA for 30 min, and then fAd for 10 min, pre-perfused with 1 μM TG for 30 min, and then fAd for 10 min, pre-perfused with EGTA combined with TG for 30 min, and then fAd for 10 min, EGTA alone, TG alone, EGTA and TG. **d** p-CaMKKβ and p-AMPK expression in the above eight groups. **e** Quantitative analysis of p-CaMKKβ expression normalized to CaMKKβ. **f** Quantitative analysis of p-AMPK expression normalized to AMPK. The values shown are means ± SD from four independent experiments. $^{*}P < 0.05$ and $^{**}P < 0.01$ compared with KRH group. $^{\#\#}P < 0.01$ compared with fAd group

SMG-C6 cells. The basal TER value of untreated monolayers was 678 ± 54.62 Ω cm^2, consistent with previous studies (Ding et al. 2013; Kawedia et al. 2008). fAd caused a rapid and significant decrease in TER value (Fig. 3a, b). Pre-treatment with either EGTA or TG did not affect fAd-induced decrease in TER value (Fig. 3c, d). However, pre-treatment with EGTA combined with TG abolished fAd decreased TER value (Fig. 3e). EGTA and/or TG alone did not affect the basal TER values (Fig. 3f–h).

Paracellular permeability can also be evaluated using 4-kDa FITC-dextran as a non-charged paracellular tracer. Results showed that the *P*app for 4-kDa FITC-dextran was greatly increased by fAd with or without EGTA/TG pre-treatment (Fig. 4a–d), whereas pre-treatment with EGTA combined with TG abolished fAd-induced increase in *P*app (Fig. 4e). EGTA and/or TG alone did not affect the basal *P*app (Fig. 4f–h). These data indicate that adiponectin regulates paracellular permeability in a Ca^{2+}-dependent manner,

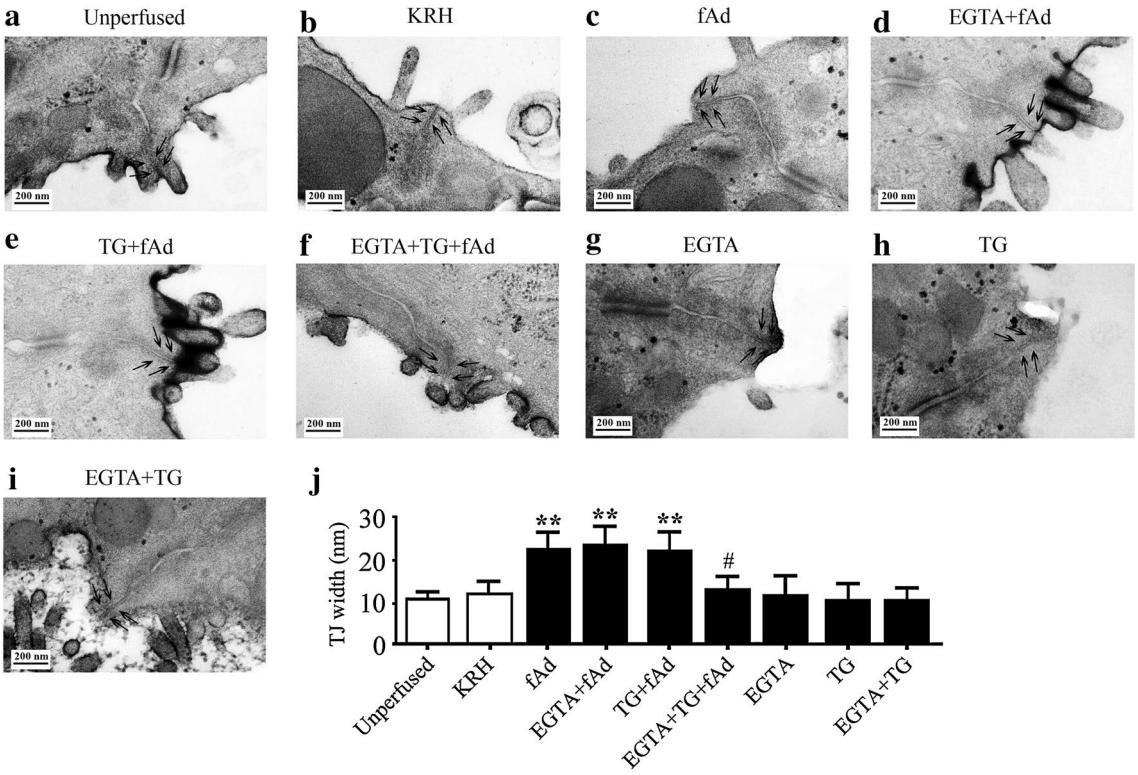

Fig. 2 Ca^{2+} is involved in adiponectin-modulated tight junction ultrastructure. Representative images of TJ structure in unperfused glands (**a**), in glands perfused with KRH (**b**), 1 μg/ml fAd for 10 min (**c**), pre-perfused with 1 μM EGTA for 30 min, and then fAd for 10 min (**d**), pre-perfused with 1 μM TG for 30 min, and then fAd for 10 min (**e**), pre-perfused with EGTA combined with TG for 30 min, and then fAd for 10 min (**f**), EGTA alone (**g**), TG alone (**h**), EGTA and TG (**i**). TJs are indicated by arrows. Bar: 200 μm. **j** The width of apical TJs was measured in ten randomly selected fields in four sections from each gland. The values shown are means ± SD from four independent experiments. $^{**}P < 0.01$ compared with the KRH group. $^{\#}P < 0.05$ compared with fAd group

and both extracellular Ca^{2+} influx and intracellular Ca^{2+} release contribute to this effect.

CaMKKβ is an upstream kinase for adiponectin-induced AMPK activation

LKB1 and CaMKKβ have been identified as upstream kinases that activate AMPK (Woods et al. 2003, 2005). To determine whether LKB1 or CaMKKβ are involved in adiponectin-induced AMPK activation in rat submandibular glands, we stimulated SMG-C6 cells with fAd for 10 min. As shown in Fig. 5a–d, fAd significantly increased the phosphorylation of CaMKKβ and AMPK, whereas LKB1 phosphorylation was not changed. These results suggest that CaMKKβ, but not LKB1, is responsible for adiponectin-induced activation of AMPK in submandibular glands.

CaMKKβ is required for adiponectin-induced secretion in submandibular glands

To further reveal the role of CaMKKβ in adiponectin-induced saliva secretion, the isolated submandibular glands were perfused with STO-609, a CaMKKβ antagonist. As shown in Fig. 5e, pre-perfusion with STO-609 (1 mM) abolished increased secretion induced by fAd, whereas STO-609 alone had no influence. Moreover, pre-perfusion with STO-609 abolished fAd-induced AMPK phosphorylation, whereas STO-609 alone did not change the level of p-AMPK (Fig. 5f, g). These results indicate that CaMKKβ might be an up-stream kinase to modulate adiponectin-promoted AMPK phosphorylation.

CaMKKβ is involved in adiponectin-modulated tight junction ultrastructure and paracellular permeability

We next examined whether CaMKKβ is involved in the modulation of TJ ultrastructure and paracellular permeability induced by adiponectin. Perfusion with fAd increased TJ width. Pre-perfusion with STO-609 abolished fAd-induced increase in TJ width, while STO-609 alone had no effect on the ultrastructure of TJs (Fig. 6a–e). These results suggest that CaMKKβ is involved in the TJ "opening" in response to adiponectin.

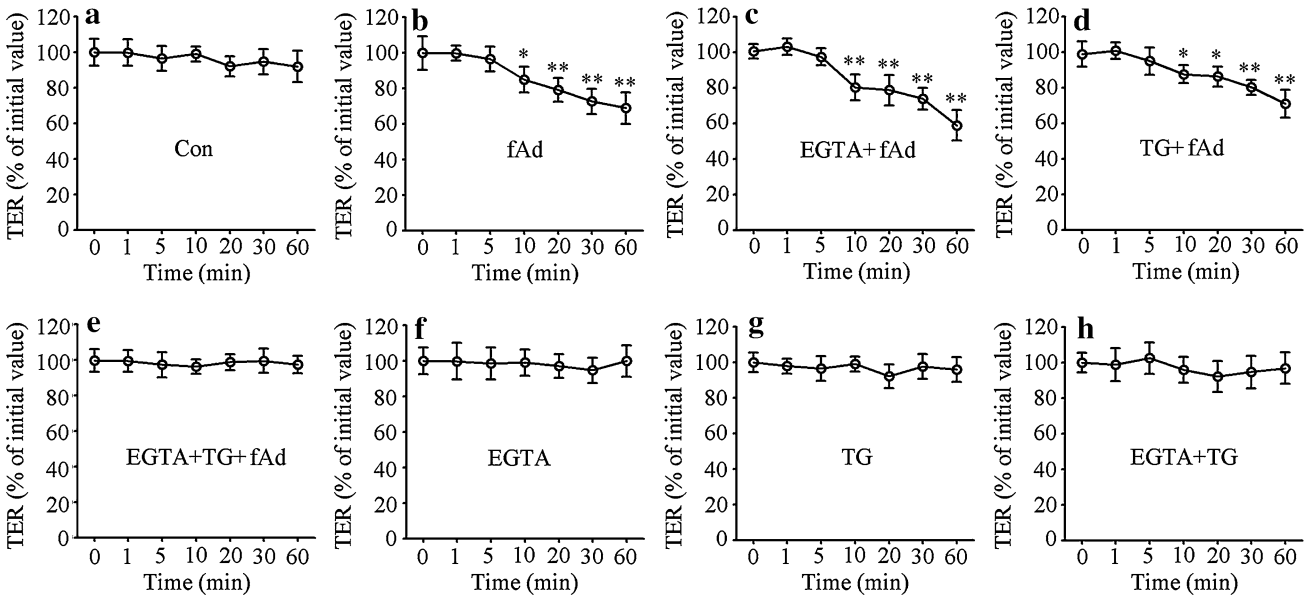

Fig. 3 Ca^{2+} is required for adiponectin-decreased TER values. The time course of transepithelial electrical resistance (TER) in SMG-C6 cells was measured using an epithelial volt ohm meter. The value of TER in untreated SMG-C6 cells (**a**), in cells incubated with 1 μg/ml fAd for 60 min (**b**), pre-incubated with 1 μM EGTA for 30 min, and then fAd for 60 min (**c**), pre-incubated with 1 μM TG, and then fAd for 60 min (**d**), pre-incubated with EGTA combined with TG, and then fAd for 60 min (**e**), EGTA alone (**f**), TG alone (**g**), EGTA and TG (**h**). The values shown are means ± SD from four independent experiments. $^{*}P<0.05$ and $^{**}P<0.01$ compared with untreated control cells

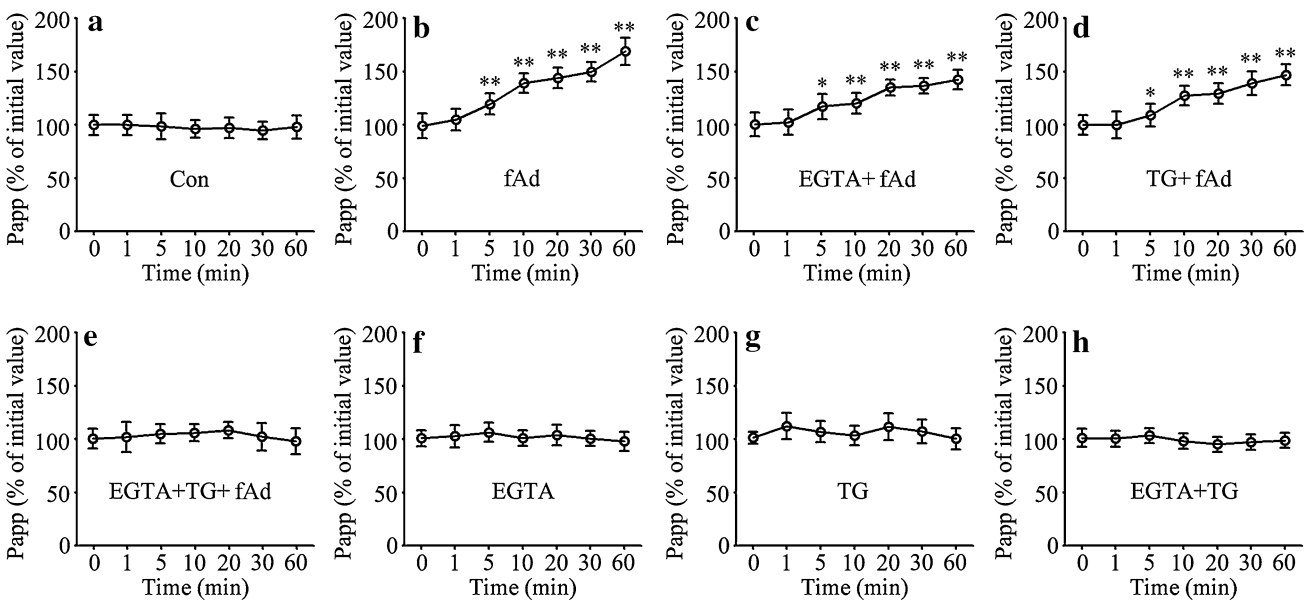

Fig. 4 Ca^{2+} is required for adiponectin-increased permeability of FITC-dextran. The apparent permeability coefficient (*P*app) of 4-kDa FITC-dextran was determined as the increase in the amount of tracer per time per filter area. The *P*app value in untreated SMG-C6 cells (**a**), in cells incubated with 1 μg/ml fAd (**b**), pre-incubated with 1 μM EGTA, and then fAd for 60 min (**c**), pre-incubated with 1 μM TG, and then fAd for 60 min (**d**), pre-incubated with EGTA combined with TG, and then fAd for 60 min (**e**), EGTA alone (**f**), TG alone (**g**), EGTA and TG (**h**). The values shown are means ± SD from four independent experiments. $^{*}P<0.05$ and $^{**}P<0.01$ compared with untreated control cells

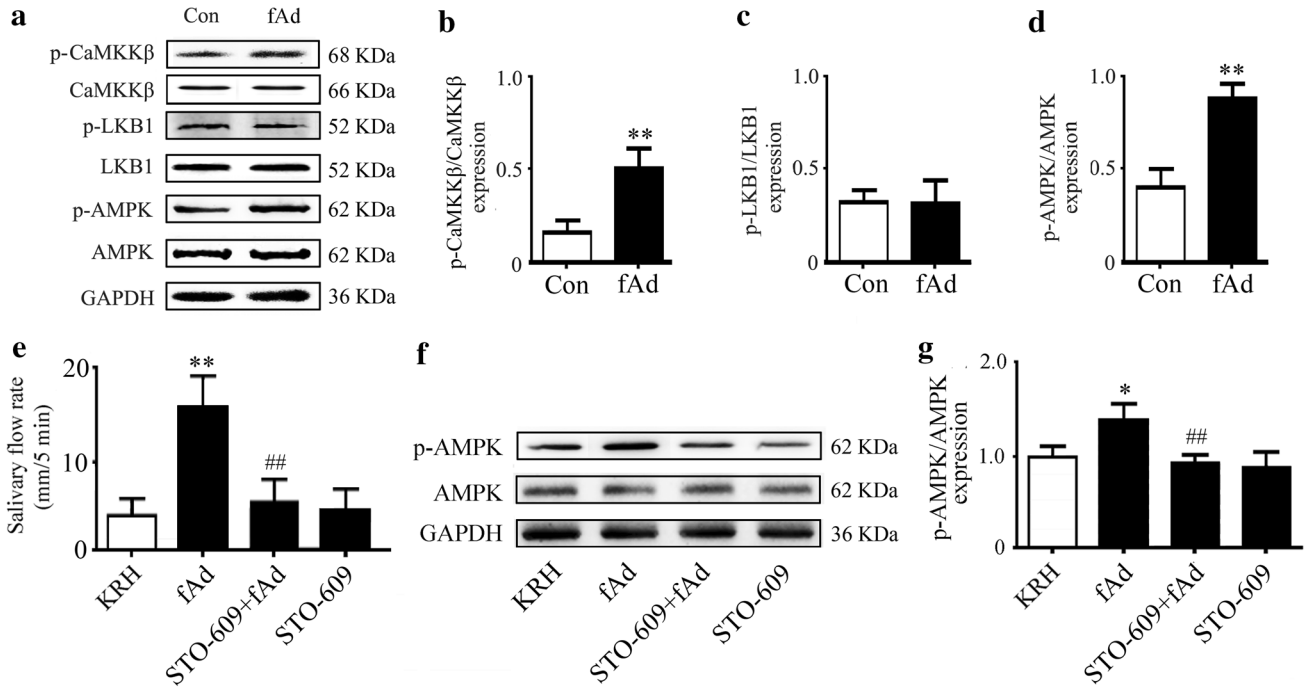

Fig. 5 CaMKKβ is required for adiponectin-induced AMPK activation and secretion in submandibular glands. **a** Expression of p-CaMKKβ, CaMKKβ, p-LKB1, LKB1, p-AMPK, and AMPK in SMG-C6 cells stimulated with 1 μg/ml fAd for 10 min. Quantitative analysis of p-CaMKKβ expression normalized to CaMKKβ (**b**), p-LKB expression normalized to LKB (**c**), p-AMPK expression normalized to AMPK (**d**). The values shown are means ± SD from four independent experiments. $^{**}P < 0.01$ compared with untreated control cells. **e** The salivary flow rate in glands perfused with KRH for 10 min, perfused with 1 μg/ml fAd for 10 min, pre-perfused with 1 mM STO-609 for 30 min, and then fAd for 10 min, STO-609 alone. The values shown are means ± SD from four independent experiments. $^{**}P < 0.01$ compared with KRH group. $^{\#\#}P < 0.05$ compared with fAd group. **f** p-AMPK expression in the above four groups. **g** Quantitative analysis of p-AMPK expression normalized to AMPK. The values shown are means ± SD from four independent experiments. $^{*}P < 0.05$ compared with KRH group. $^{\#\#}P < 0.05$ compared with fAd group

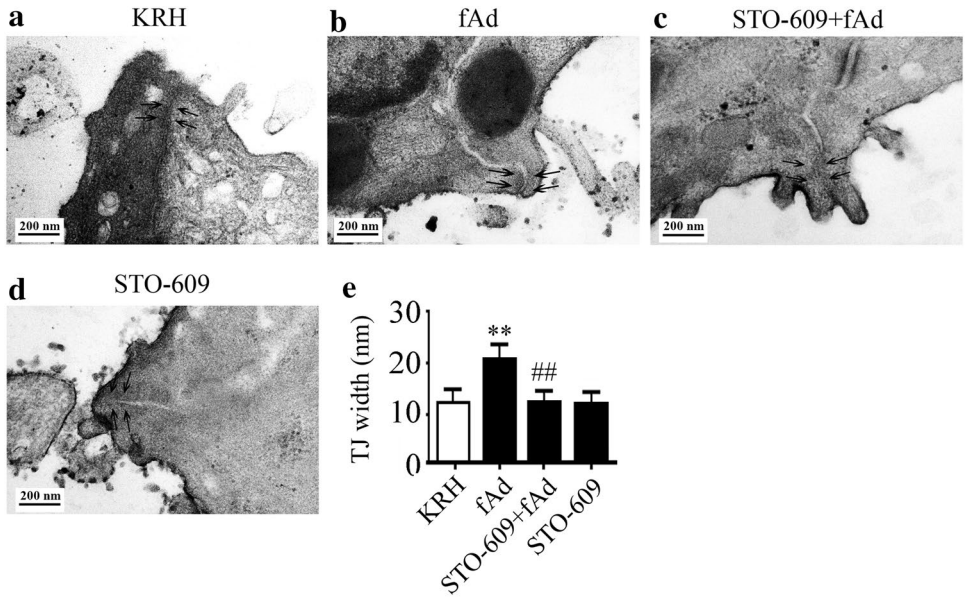

Fig. 6 CaMKKβ is involved in adiponectin-modulated tight junction ultrastructure. Representative images of TJ in glands perfused with KRH (**a**), perfused with 1 μg/ml fAd for 10 min (**b**), pre-perfused with 1 mM STO-609 for 30 min, and then fAd for 10 min (**c**), perfused with STO-609 alone (**d**). TJs are indicated by arrows. Bar: 200 μm. **e** The width of apical TJs was measured in ten randomly selected fields in four sections from each gland. The values shown are means ± SD from four independent experiments. $^{**}P < 0.01$ compared with KRH group. $^{\#\#}P < 0.05$ compared with KRH group

To confirm the role of CaMKKβ in adiponectin-modulated paracellular permeability, we knockdown CaMKKβ expression by transfection with CaMKKβ shRNA and then rescued its expression by CaMKKβ cDNA into SMG-C6 cells. As shown in Fig. 7a, the expression of CaMKKβ protein was decreased in CaMKKβ shRNA-transfected cells, and increased in CaMKKβ cDNA-transfected cells. As shown in Fig. 7b, transfection with CaMKKβ shRNA did not affect the basal TER value. fAd-decreased TER values (Fig. 7c) were abolished in CaMKKβ-knockdown cells (Fig. 7d). Furthermore, fAd-mediated decrease in TER values was reappeared in CaMKKβ rescued cells (Fig. 7e). Paracellular permeability assay was also performed using FITC-dextran, and the results showed that knockdown of CaMKKβ abolished and rescue of CaMKKβ reappeared fAd-induced *P*app increase (Fig. 8a–e). These results indicate that adiponectin increases paracellular permeability in a CaMKKβ-dependent manner.

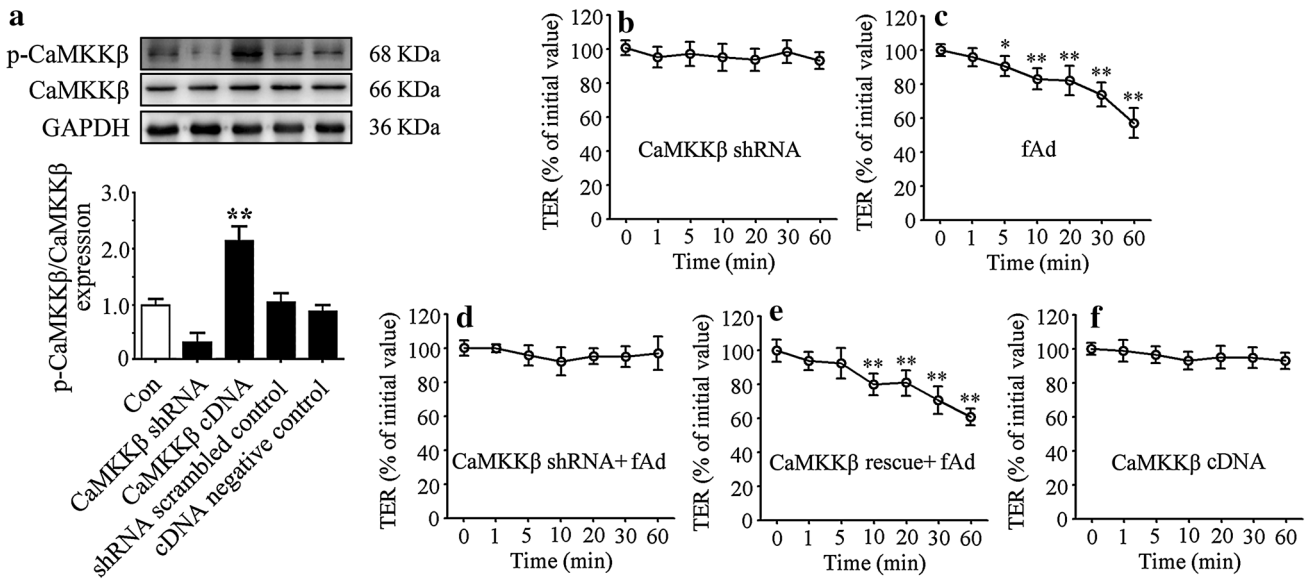

Fig. 7 CaMKKβ is required for adiponectin-decreased TER values. **a** Expressions of p-CaMKKβ and CaMKKβ in SMG-C6 cells transfected with CaMKKβ shRNA and CaMKKβ cDNA. $^{**}P<0.01$ compared with untransfected control cells. The basal TER value in SMG-C6 cells transfected with CaMKKβ shRNA alone (**b**), in cells incubated with 1 μg/ml fAd for 60 min (**c**), transfected with CaMKKβ shRNA, and then fAd for 60 min (**d**), rescued with CaMKKβ cDNA, and then fAd for 60 min (**e**), CaMKKβ cDNA alone (**f**). The values shown are means ± SD from four independent experiments. $^{*}P<0.05$ and $^{**}P<0.01$ compared with untreated control cells

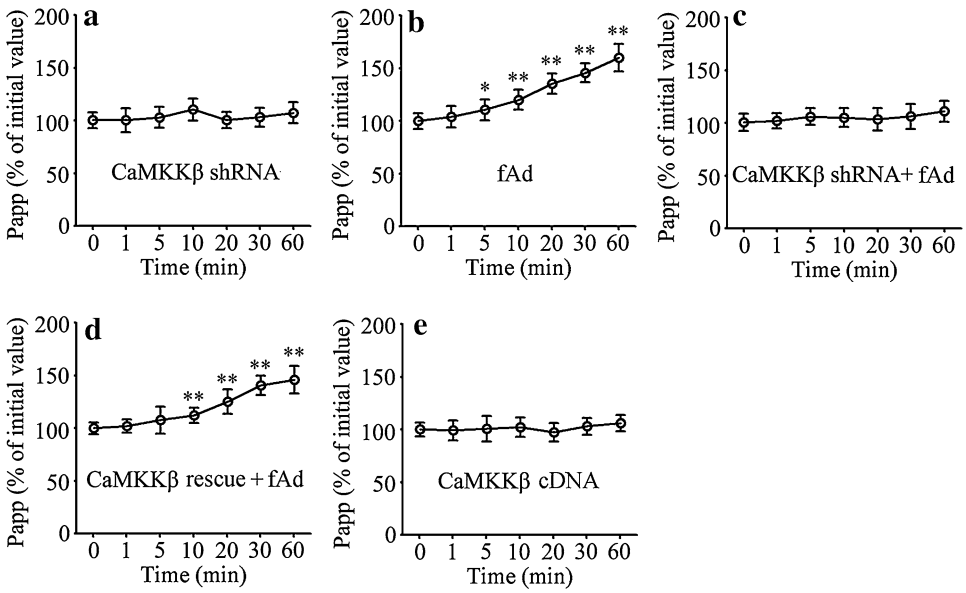

Fig. 8 CaMKKβ is required for adiponectin-increased permeability of FITC-dextran. The basal *P*app value in SMG-C6 cells transfected with CaMKKβ shRNA alone (**a**), in cells incubated with 1 μg/ml fAd for 60 min (**b**), transfected with CaMKKβ shRNA, and then fAd for 60 min (**c**), rescued with CaMKK β cDNA, and then fAd for 60 min (**d**), CaMKKβ cDNA alone (**e**). The values shown are means ± SD from four independent experiments. $^{*}P<0.05$ and $^{**}P<0.01$ compared with untreated control cells

Discussion

In the present study, we demonstrated that adiponectin increased Ca^{2+} modulation in rat submandibular glands acinar cells. Both extracellular Ca^{2+} influx and release of Ca^{2+} from endoplasmic reticulum were involved in adiponectin-induced salivary secretion, activation of AMPK, and increase in paracellular permeability. Moreover, CaMKKβ activated by increased $[Ca^{2+}]_i$, but not by LKB1, acted as an upstream kinase for adiponectin-mediated AMPK activation. Inhibition of CaMKKβ by pharmacological reagent or CaMKKβ shRNA abolished, whereas CaMKKβ re-expression retained, the increase in TJ width and paracellular permeability induced by fAd. These results reveal that the Ca^{2+}-CaMKKβ pathway is responsible for adiponectin-induced salivary secretion via activation of AMPK and increase in paracellular permeability in rat submandibular glands.

In rat pituitary cells, adiponectin increases $[Ca^{2+}]_i$ through both the influx of extracellular Ca^{2+} and the release of Ca^{2+} from endoplasmic reticulum resulting in the secretion of growth hormone (Steyn et al. 2009). In C2C12 myocytes and Xenopus oocytes, adiponectin induced extracellular Ca^{2+} influx via adiponectin receptor 1. Inhibition of Ca^{2+} influx is associated with insulin resistance and reduced exercise tolerance due to the decreased adiponectin levels (Iwabu et al. 2010). In addition, adiponectin-induced increased Ca^{2+} influx is also involved in adrenal cortical hormone release in pituitary cells (Chen et al. 2014). In human and rabbit submandibular glands, activation of mAChRs and transient receptor potential vanilloid subtype 1 increase salivary secretion through elevated $[Ca^{2+}]_i$ (Ding et al. 2014; Zhang et al. 2006). Moreover, in human transplanted epiphora submandibular glands, the increased $[Ca^{2+}]_i$ mobilization induced by mAChR activation contributes to hyperscretion (Ding et al. 2014). However, adiponectin-promoted salivary secretion in rat submandibular glands is independent of cholinergic manner (Ding et al. 2013). In the present study, we found that adiponectin could induce increase in $[Ca^{2+}]_i$ in isolated rat submandibular gland acinar cells. Either EGTA or TG did not affect the adiponectin-induced salivary secretion, however, co-inhibition of extracellular Ca^{2+} influx and intracellular Ca^{2+} release from endoplasmic reticulum completely abolished adiponectin-induced salivary secretion. These results identify that the elevated $[Ca^{2+}]_i$, derived from both extracellular Ca^{2+} influx and intracellular Ca^{2+} release, is required for the adiponectin-induced salivary secretion in submandibular glands.

The secretion of saliva across the salivary epithelium can be accomplished via either aquaporin 5-based transcellular route or TJ-based paracellular route (Kawedia et al. 2007). We previously demonstrated that adiponectin-induced salivary secretion in rat submandibular glands involves modulation of paracellular permeability through TJs, but not mediated by aquaporin 5 (Ding et al. 2013). TJs, which consist of a narrow belt-like structure at the most apical portion of the lateral membranes, serve as an indispensable gate for the transport of materials through paracellular pathway (Tsukita et al. 2001). Secretory stimulators, such as carbachol and capsaicin are reported to induce salivation by altering TJ properties and increasing paracellular permeability (Cong et al. 2013, 2015; Ding et al. 2013, 2017; Yang et al. 2017). Moreover, proinflammatory cytokines change TJ content and disrupt TJ barrier function, which might be the mechanism for the hyposecretion that occurs in Sjögren's syndrome (Abe et al. 2016; Baker et al. 2008; Ewert et al. 2010; Mei et al. 2015; Zhang et al. 2016). In rat submandibular glands, adiponectin increases TJ width and paracellular permeability (Ding et al. 2013). Furthermore, AMPK activation regulates the content and distribution of TJ components, resulting in an increased paracellular permeability and salivary secretion (Xiang et al. 2014). Here, inhibition of either extracellular Ca^{2+} influx or Ca^{2+} released from endoplasmic reticulum did not affect adiponectin-induced increase in TJ width in isolated rat submandibular glands. However, co-inhibition of Ca^{2+} influx and Ca^{2+} release from endoplasmic reticulum abolished the adiponectin-induced increased TJ width. Furthermore, in SMG-C6 cells, EGTA combination with TG abolished increased paracellular permeability induced by adiponectin. These results indicate that both Ca^{2+} influx and Ca^{2+} release from endoplasmic reticulum participate in adiponectin-induced salivary secretion via regulating TJ ultrastructure and function.

AMPK is controlled by two upstream kinases, LKB1 and CaMKKβ (Hawley et al. 2005; Woods et al. 2003). In Alzheimer's disease, the CaMKKβ-AMPK pathway plays a major role in mediating the early synaptotoxic effects of amyloid-β1-42 oligomers both in vitro and in vivo, serving as a potential therapeutic target for Alzheimer's disease (Mairet-Coello et al. 2013). In human pancreatic tumor cells, 2-deoxyglucose-induced endoplasmic reticulum stress results in an increased Ca^{2+} leakage from endoplasmic reticulum, which subsequently activates AMPK via CaMKKβ and ultimately leads to cell autophagy (Xi et al. 2013). In HeLa cells, the increased $[Ca^{2+}]_i$ activates CaMKKβ-AMPK pathway, which participates in the protective effect of *baicalin* against the development of hepatic steatosis and obesity in vivo (Ma et al. 2012). However, whether LKB1 and/or CaMKKβ are involved in adiponectin-mediated AMPK activation in submandibular glands is not determined. Here, we found that adiponectin induced AMPK activation by increasing phosphorylation of CaMKKβ, but not LKB1 phosphorylation, suggesting that CaMKKβ, but not LKB1, is the

upstream kinase for adiponectin-mediated AMPK activation in rat submandibular glands. Furthermore, co-inhibition of Ca^{2+} influx and Ca^{2+} release from endoplasmic reticulum abolished adiponectin-induced CaMKKβ and AMPK activation and salivary secretion. These results suggest that Ca^{2+}-CaMKKβ-AMPK signaling pathway is involved in adiponectin-modulated salivary secretion. In SMG-C6 cells, CaMKKβ knockdown did not alter basal TER or *P*app values, suggesting that the maintenance of basal paracellular permeability does not require CaMKKβ involvement. However, increased paracellular permeability induced by adiponectin was inhibited by CaMKKβ-knockdown, whereas re-expression of CaMKKβ rescued the effect of adiponectin. These results suggest that Ca^{2+}-CaMKKβ pathway is involved in adiponectin-modulated paracellular permeability in rat submandibular glands.

In summary, our results provide evidence that Ca^{2+}- and CaMKKβ-mediated AMPK activation is required for adiponectin-induced salivary secretion. Our findings will enrich our understanding of the secretory mechanisms that link adiponectin to saliva secretion by regulating Ca^{2+} modulation and paracellular permeability.

Acknowledgements This study was supported by the National Natural Science Foundation of China 81771088 (CD), 81200799 (CD) and Tai Sheng Dental Medicine Development Fund (GYY).

Author contributions CD performed the major experiments and wrote the manuscript. ZHD and SLL participated in data interpretation and manuscript improvement. LLW and GYY designed the study, analyzed the data, and wrote the manuscript. All authors read and approved the final manuscript.

Compliance with ethical standards

Conflict of interest The authors declare that they have no competing interests.

References

Abe A, Takano K, Kojima T, Nomura K, Kakuki T, Kaneko Y, Yamamoto M, Takahashi H, Himi T (2016) Interferon-gamma increased epithelial barrier function via upregulating claudin-7 expression in human submandibular gland duct epithelium. J Mol Histol 47(3):353–363. https://doi.org/10.1007/s10735-016-9667-2

Baker OJ, Camden JM, Redman RS, Jones JE, Seye CI, Erb L, Weisman GA (2008) Proinflammatory cytokines tumor necrosis factor-alpha and interferon-gamma alter tight junction structure and function in the rat parotid gland Par-C10 cell line. Am J Physiol Cell Physiol 295:C1191–1201. https://doi.org/10.1152/ajpcell.00144.2008

Baum BJ (1993) Principles of saliva secretion. Ann N Y Acad Sci 694:17–23. https://doi.org/10.1111/j.1749-6632.1993.tb18338.x

Chen M, Wang Z, Zhan M, Liu R, Nie A, Wang J, Ning G, Ma Q (2014) Adiponectin regulates ACTH secretion and the HPAA in an AMPK-dependent manner in pituitary corticotroph cells. Mol Cell Endocrinol 383(1–2):118–125. https://doi.org/10.1016/j.mce.2013.12.007

Cong X, Zhang Y, Yang NY, Li J, Ding C, Ding QW, Su YC, Mei M, Guo XH, Wu LL, Yu GY (2013) Occludin is required for TRPV1-modulated paracellular permeability in the submandibular gland. J Cell Sci 126(Pt 5):1109–1121. https://doi.org/10.1242/jcs.111781

Cong X, Zhang Y, Li J, Mei M, Ding C, Xiang RL, Zhang LW, Wang Y, Wu LL, Yu GY (2015) Claudin-4 is required for modulation of paracellular permeability by muscarinic acetylcholine receptor in epithelial cells. J Cell Sci 128(12):2271–2286. https://doi.org/10.1242/jcs.165878

Coronado R, Morrissette J, Sukhareva M, Vaughan DM (1994) Structure and function of ryanodine receptors. Am J Physiol 266(6 Pt 1):C1485–C1504

Ding C, Li L, Su YC, Xiang RL, Cong X, Yu HK, Li SL, Wu LL, Yu GY (2013) Adiponectin increases secretion of rat submandibular gland via adiponectin receptors-mediated AMPK signaling. PLoS ONE 8(5):e63878. https://doi.org/10.1371/journal.pone.0063878

Ding C, Cong X, Zhang Y, Yang NY, Li SL, Wu LL, Yu GY (2014) Hypersensitive mAChRs are involved in the epiphora of transplanted glands. J Dent Res 93(3):306–312. https://doi.org/10.1177/0022034513519107

Ding C, Cong X, Zhang XM, Li SL, Wu LL, Yu GY (2017) Decreased interaction between ZO-1 and occludin is involved in alteration of tight junctions in transplanted epiphora submandibular glands. J Mol Histol 48(3):225–234. https://doi.org/10.1007/s10735-017-9716-5

Evans RL, Turner RJ (1997) Upregulation of Na(+)-K(+)-2Cl- cotransporter activity in rat parotid acinar cells by muscarinic stimulation. J Physiol 499:351–359

Ewert P, Aguilera S, Alliende C, Kwon YJ, Albornoz A, Molina C, Urzua U, Quest A, Olea N, Perez P, Castro I, Barrera MJ, Romo R, Hermoso M, Leyton C, Gonzalez MJ (2010) Disruption of tight junction structure in salivary glands from Sjögren's syndrome patients is linked to proinflammatory cytokine exposure. Arthritis Rheum 62(5):1280–1289. https://doi.org/10.1002/art.27362

Garrett JR, Ekström J, Anderson LC (1999) Neural mechanisms of salivary gland secretion. Front Oral Biol. Basel, Karger, pp 231–236

Giovannucci DR, Bruce JI, Straub SV, Arreola J, Sneyd J, Shuttleworth TJ, Yule DI (2002) Cytosolic Ca(2+) and Ca(2+)-activated Cl(-) current dynamics: insights from two functionally distinct mouse exocrine cells. J Physiol 540(Pt 2):469–484. https://doi.org/10.1113/jphysiol.2001.013453

Hawley SA, Boudeau J, Reid JL, Mustard KJ, Udd L, Makela TP, Alessi DR, Hardie DG (2003) Complexes between the LKB1 tumor suppressor, STRAD alpha/beta and MO25 alpha/beta are upstream kinases in the AMP-activated protein kinase cascade. J Biol 2(4):28. https://doi.org/10.1186/1475-4924-2-28

Hawley SA, Pan DA, Mustard KJ, Ross L, Bain J, Edelman AM, Frenguelli BG, Hardie DG (2005) Calmodulin-dependent protein kinase kinase-beta is an alternative upstream kinase for AMP-activated protein kinase. Cell Metab 2(1):9–19. https://doi.org/10.1016/j.cmet.2005.05.009

Ishikawa Y, Eguchi T, Skowronski MT, Ishida H (1998) Acetylcholine acts on M3 muscarinic receptors and induces the translocation of aquaporin5 water channel via cytosolic Ca^{2+} elevation in rat parotid glands. Biochem Biophys Res Commun 245(3):835–840. https://doi.org/10.1006/bbrc.1998.8395

Iwabu M, Yamauchi T, Okada-Iwabu M, Sato K, Nakagawa T, Funata M, Yamaguchi M, Namiki S, Nakayama R, Tabata M, Ogata H, Kubota N, Takamoto I, Hayashi YK, Yamauchi N, Waki H, Fukayama M, Nishino I, Tokuyama K, Ueki K, Oike Y, Ishii S, Hirose K, Shimizu T, Touhara K, Kadowaki T (2010) Adiponectin and AdipoR1 regulate PGC-1alpha and mitochondria by Ca(2+) and AMPK/SIRT1. Nature 464(7293):1313–1319. https://doi.org/10.1038/nature08991

Joseph SK (1996) The inositol triphosphate receptor family. Cell Signal 8(1):1–7. https://doi.org/10.1016/0898-6568(95)02012-8

Kaplan MD, Baum BJ (1993) The functions of saliva. Dysphagia 8(3):225–229

Kawedia JD, Nieman ML, Boivin GP, Melvin JE, Kikuchi K, Hand AR, Lorenz JN, Menon AG (2007) Interaction between transcellular and paracellular water transport pathways through aquaporin 5 and the tight junction complex. Proc Natl Acad Sci USA 104(9):3621–3626. https://doi.org/10.1073/pnas.0608384104

Kawedia JD, Jiang M, Kulkarni A, Waechter HE, Matlin KS, Pauletti GM, Menon AG (2008) The protein kinase A pathway contributes to Hg^{2+}-induced alterations in phosphorylation and subcellular distribution of occludin associated with increased tight junction permeability of salivary epithelial cell monolayers. J Pharmacol Exp Ther 326(3):829–837. https://doi.org/10.1124/jpet.107.135798

Liu X, O'Connell A, Ambudkar IS (1998) Ca^{2+}-dependent inactivation of a store-operated Ca^{2+} current in human submandibular gland cells. Role of a staurosporine-sensitive protein kinase and the intracellular Ca^{2+} pump. J Biol Chem 273(50):33295–33304. https://doi.org/10.1074/jbc.273.50.33295

Ma Y, Yang F, Wang Y, Du Z, Liu D, Guo H, Shen J, Peng H (2012) CaMKKbeta is involved in AMP-activated protein kinase activation by baicalin in LKB1 deficient cell lines. PLoS ONE 7(10):e47900. https://doi.org/10.1371/journal.pone.0047900

Mairet-Coello G, Courchet J, Pieraut S, Courchet V, Maximov A, Polleux F (2013) The CAMKK2-AMPK kinase pathway mediates the synaptotoxic effects of Abeta oligomers through Tau phosphorylation. Neuron 78(1):94–108. https://doi.org/10.1016/j.neuron.2013.02.003

Manganel M, Turner RJ (1990) Agonist-induced activation of Na^+/H^+ exchange in rat parotid acinar cells is dependent on calcium but not on protein kinase C. J Biol Chem 265(8):4284–4289

Mei M, Xiang RL, Cong X, Zhang Y, Li J, Yi X, Park K, Han JY, Wu LL, Yu GY (2015) Claudin-3 is required for modulation of paracellular permeability by TNF-alpha through ERK1/2/slug signaling axis in submandibular gland. Cell Signal 27(10):1915–1927. https://doi.org/10.1016/j.cellsig.2015.07.002

Nauntofte B, Poulsen JH (1986) Effects of Ca^{2+} and furosemide on Cl^- transport and O_2 uptake in rat parotid acini. Am J Physiol 251(2 Pt 1):C175–C185

Nehrke K, Quinn CC, Begenisich T (2003) Molecular identification of Ca^{2+}-activated K^+ channels in parotid acinar cells. Am J Physiol Cell Physiol 284(2):C535–C546. https://doi.org/10.1152/ajpcell.00044.2002

Nguyen HV, Stuart-Tilley A, Alper SL, Melvin JE (2004) Cl(-)/HCO(3)(−) exchange is acetazolamide sensitive and activated by a muscarinic receptor-induced [Ca(2+)](i) increase in salivary acinar cells. Am J Physiol Gastrointest Liver Physiol 286(2):G312–G320. https://doi.org/10.1152/ajpgi.00158.2003

Quissell DO, Barzen KA, Gruenert DC, Redman RS, Camden JM, Turner JT (1997) Development and characterization of SV40 immortalized rat submandibular acinar cell lines. In Vitro Cell Dev Biol Anim 33(3):164–173. https://doi.org/10.1007/s11626-997-0137-8

Shibata R, Sato K, Pimentel DR, Takemura Y, Kihara S, Ohashi K, Funahashi T, Ouchi N, Walsh K (2005) Adiponectin protects against myocardial ischemia-reperfusion injury through AMPK- and COX-2-dependent mechanisms. Nat Med 11:1096–1103. https://doi.org/10.1038/nm1295

Steyn FJ, Boehme F, Vargas E, Wang K, Parkington HC, Rao JR, Chen C (2009) Adiponectin regulate growth hormone secretion via adiponectin receptor mediated Ca(2+) signaling in rat somatotrophs in vitro. J Neuroendocrinol 21(8):698–704. https://doi.org/10.1111/j.1365-2826.2009.01887.x

Tsukita S, Furuse M, Itoh M (2001) Multifunctional strands in tight junctions. Nat Rev Mol Cell Biol 2(4):285–293. https://doi.org/10.1038/35067088

Woods A, Johnstone SR, Dickerson K, Leiper FC, Fryer LG, Neumann D, Schlattner U, Wallimann T, Carlson M, Carling D (2003) LKB1 is the upstream kinase in the AMP-activated protein kinase cascade. Curr Biol 13(22):2004–2008. https://doi.org/10.1016/j.cub.2003.10.031

Woods A, Dickerson K, Heath R, Hong SP, Momcilovic M, Johnstone SR, Carlson M, Carling D (2005) Ca^{2+}/calmodulin-dependent protein kinase kinase-beta acts upstream of AMP-activated protein kinase in mammalian cells. Cell Metab 2(1):21–33. https://doi.org/10.1016/j.cmet.2005.06.005

Xi H, Barredo JC, Merchan JR, Lampidis TJ (2013) Endoplasmic reticulum stress induced by 2-deoxyglucose but not glucose starvation activates AMPK through CaMKKbeta leading to autophagy. Biochem Pharmacol 85(10):1463–1477. https://doi.org/10.1016/j.bcp.2013.02.037

Xiang RL, Mei M, Cong X, Li J, Zhang Y, Ding C, Wu LL, Yu GY (2014) Claudin-4 is required for AMPK-modulated paracellular permeability in submandibular gland cells. J Mol Cell Biol 6(6):486–497. https://doi.org/10.1093/jmcb/mju048

Yamauchi T, Kamon J, Minokoshi Y, Ito Y, Waki H, Uchida S, Yamashita S, Noda M, Kita S, Ueki K, Eto K, Akanuma Y, Froguel P, Foufelle F, Ferre P, Carling D, Kimura S, Nagai R, Kahn BB, Kadowaki T (2002) Adiponectin stimulates glucose utilization and fatty-acid oxidation by activating AMP activated protein kinase. Nat Med 8:1288–1295. https://doi.org/10.1038/nm788

Yang NY, Ding C, Li J, Zhang Y, Xiang RL, Wu LL, Yu GY, Cong X (2017) Muscarinic acetylcholine receptor-mediated tight junction opening is involved in epiphora in late phase of submandibular gland transplantation. J Mol Histol 48(2):99–111. https://doi.org/10.1007/s10735-016-9709-9

Zhang GH, Wells J, Willis S, Martinez JR (1996) Evidence for reduced capacity for Ca^{2+} removal from the cytosol in submandibular cells of newborn rats. Biochem Biophys Res Commun 228(1):171–175. https://doi.org/10.1006/bbrc.1996.1634

Zhang Y, Xiang B, Li YM, Wang Y, Wang X, Wang YN, Wu LL, Yu GY (2006) Expression and characteristics of vanilloid receptor 1 in the rabbit submandibular gland. Biochem Biophys Res Commun 345(1):467–473. https://doi.org/10.1016/j.bbrc.2006.04.106

Zhang LW, Cong X, Zhang Y, Wei T, Su YC, Serrão AC, Brito AR Jr, Yu GY, Hua H, Wu LL (2016) Interleukin-17 impairs salivary tight junction integrity in Sjögren's syndrome. J Dent Res 95(7):784–792. https://doi.org/10.1177/0022034516634647